Research and Reviews in Materials Science and Chemistry
Vol. 5, Issue 1, 2015, Pages 63-78
ISSN 2319-6920
Published Online on July 31, 2015

http://jyotiacademicpress.net

SYNTHESIS AND CHARACTERIZATION OF POLYMER-TELLURIUM CHAIN-LIKE NANOSTRUCTURES COMPOSITE THIN FILM

FILIPPO EMANUELA[1], TEPORE MARCO[1], QUARTA GIANLUCA[1], CALCAGNILE LUCIO[1], RELLA ROBERTO[2], MANERA MARIA GRAZIA[2] and ANTONIO TEPORE[3]

[1]Department of Engineering for Innovation
University of Salento
Monteroni Street, Lecce I-73100
Italy
e-mail: emanuela.filippo@unisalento.it

[2]CNR-IMM Institute for Microelectronic and Microsystems
Unit of Lecce, Monteroni Street
Lecce I-73100
Italy

[3]Department of Cultural Heritage
University of Salento
Lecce I-73100
Italy

Abstract

Thin film composites consisting of tellurium chain-like nanostructures embedded in a poly vinyl alcohol (PVA) matrix, were prepared using a two step approach. In the first step, tellurium nanoparticles which self-assembled into

Keywords and phrases: oxide nanoparticles, vapour deposition, XRD, TEM, sensor.
Communicated by Ana Rosa Silva.
Received February 5, 2015

nanochains have been prepared in high yield through thermal evaporation and deposition of Te bulk powder in a horizontal tube furnace. The obtained nanochains were characterized by X-ray diffraction, transmission electron microscopy, UV-Vis, and Raman spectroscopy. Experimental results evidenced that Te nanoparticles with a diameter in the range 40-100nm assembled spontaneously to form novel chain-like nanostructures 200-600nm in length. In a second step, PVA-Te nanochains composite thin films have been prepared by spin-coating the aqueous solution of the polymer and the pre-synthesized Te nanochains. The optical gas sensing properties of such a novel hybrid composite film were tested upon exposure to volatile organic compounds samples, as methanol, ethanol, and 2-propanol.

1. Introduction

Composites consisting of polymers with embedded inorganic nanostructures have become a prominent area of current research for novel applications such as fabrication of nanodevices, gas sensors, and biosensors. The combination of inorganic nanostructures and a polymer provides a simple route to stable and processable composite materials, integrating the properties of both components. The synthesis of such nanocomposites typically involves the deposition of nanostructures into a dielectric matrix. Polymeric matrix is particularly interesting because it is low-cost and easily processable. Moreover, the properties of such composites are closely related to the kind and to the morphology of the embedded nanostructures. These composites materials exhibit unique optical characteristics originating from the strong interaction between incident light and embedded nanostructures. This interaction results in collective oscillation of electron clouds, called surface plasmons, at the interface of the nanostructures and the polymer matrix [1].

Trigonal tellurium (t-Te) nanostructures have recently become the focus of scientific efforts because it is a valuable *p*-type narrow-band gap material with good photoconductivity, photoelectricity, thermoelectricity, catalytical and nonlinear optical properties, and high piezoelectricity [2]. Furthermore, due to its highly anisotropic crystalline structure, the system favours 1D nanostructured growth. Among the various reported methods for the synthesis of Te nanostructures, vapour-phase synthesis is probably one of the most widely used, although so far it has been mainly employed for the synthesis of nanowires and nanotubes [3].

Nevertheless, to the best of our knowledge, the research on novel hierarchical Te structures with different morphologies has been still limited. The formation of flower-like, spherical, ball flower, nest-like and sheet tellurium nanostructures has been achieved only through complex and long solution phase procedures [4]. Hence, it is desirable to develop simple route for the synthesis of novel tellurium nanostructures [5].

In our previous work, single crystalline tellurium microtubes could be easily produced through vapour deposition route [6]. In this paper, we report a convenient, efficient, free of any templates or crystal seeds synthesis of good quality crystalline Te nanoparticles which self-assembled into nanochains, using the vapour deposition method at an evaporation temperature of 500°C and a deposition temperature of 100°C. A possible explanation for the self-assembly process has been proposed on the basis of the experimental observations. In a second step of our experiments, an environmentally benign approach has been proposed for the preparation of free standing poly vinyl alcohol (PVA) -Te nanochains composite thin films. The film thickness of the Te-PVA film spin-coated on a substrate was measured by using a profilometer. The polymer serves as binder between nanochains and any substrate. Composite thin films containing nanostructures could be useful in a wide range of applications, including catalysis and sensing. In this work, the optical gas sensing properties of polymer-tellurium nanochains composite film were tested upon exposure to volatile organic compounds vapour samples, as methanol, ethanol, and 2-propanol.

2. Experimental

2.1. Materials and methods

Tellurium nanostructures were synthesized by thermal evaporation of tellurium powder in argon atmosphere flow. In detail, tellurium powder (purity 99.99%) was placed in a quartz boat, which was placed at the center of a horizontal tube furnace. Tellurium was directly evaporated onto quartz substrates placed 20cm far away, downstream

inside the tube. The furnace was rapidly ramped up to 500ºC with an increasing rate of 20ºC min^{-1} and kept at this temperature for 60 min. Afterwards, the furnace was naturally cooled down to room temperature. During all the experiment, the flow rate of argon was kept constant at 100 sccm. Grayish-black films were deposited all over the substrate. The obtained nanostructures were characterized by X-ray diffraction (XRD), transmission electron microscopy (TEM), Raman and UV-Vis spectroscopy. X-ray diffraction measurements were carried out in the reflection mode on a Mini Flex Rigaku model diffractometer with CuKα radiation (λ = 0.154056nm). The X-ray diffraction data were collected at a scanning rate of 0.02º per second in 2θ ranging from 15º to 75º. The morphology of the as-grown sample was carefully investigated by using a transmission electron Hitachi H-7100 microscope operated at an accelerating voltage of 100kV. Raman scattering measurements were obtained by backscattering geometry with a Renishaw spectrometer coupled to a Leica metallo-graphic microscope. An argon-ion laser was used as excitation source. UV-Vis spectra were recorded using a Varian Cary 5 spectrophotometer. To prepare the samples for UV-Vis spectroscopic measurements and TEM observations, the synthesized nanostructures were dispersed in ethanol. A little amount of ethanol was dropped onto a carbon coated copper grid and let to dry slowly in air.

2.2. Preparation of PVA-Te composite thin film

In detail, 0.2g of PVA was dissolved in 50cm^3 of deionized water at 80ºC for 2h. The mixture was kept at room temperature for 1h in order to obtain a uniform solution. Tellurium nanostructures (150μg) were dipped into the solution at 50ºC for 1h and then the PVA-Te mixture was ultrasonicated to ensure the homogeneous dispersion of nanostructures in the polymeric matrix. This solution was used to deposit film on quartz substrate by spin-coating (at 8000rpm for 10s). The film was heat treated at 80ºC for 30 min. The obtained film had an average thickness of 0.75μm.

Optical sensing tests of the PVA-Te nanocomposite films were performed by using a home-made experimental set-up, which was designed in order to acquire the dynamic optical responses of the sensing layer to different gases and/or vapours in fixed spectral ranges. All measurements were carried out at room temperature, at 35-40% relative humidity and at normal incidence of the light beam.

3. Results

3.1. Structural and morphological characterization of Te nanochains

The crystal structure and phase composition of the obtained Te product were characterized by using X-ray powder diffraction (XRD). Figure 1 displays a representative XRD pattern of the hexagonal phase of Te crystal (cell constants $a = b = 0.4558$, $c = 5.9268$; JCPDS 65 - 3370), indicating the high crystallinity of synthesized samples.

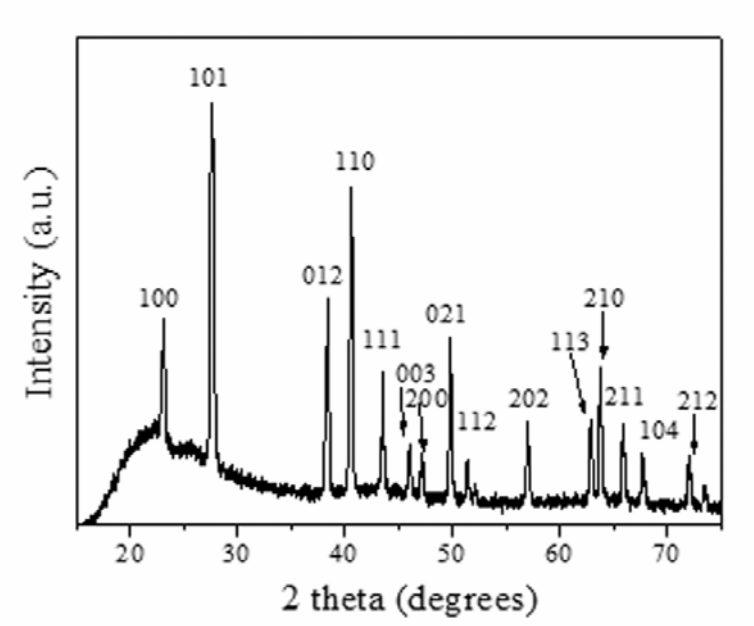

Figure 1. Typical XRD pattern of the as-synthesized Te product.

A low magnification TEM of the as-prepared Te nanostructures is shown in Figure 2. It is evident that nearly uniform nanoparticles with diameter in the range 40-100nm were obtained and that they assembled spontaneously to form novel chain-like nanostructures. These Te chain-like structures were 200-600nm in length and they have not been yet reported in literature through PVD route. TEM images clearly indicate the formation of linear and branched nanochains and that the nanoparticles connecting each other exhibit a rough surface. Some bigger nanoparticles (~200nm) with growing nanorods extruding from their surfaces could also be observed (Figure 2(a)).

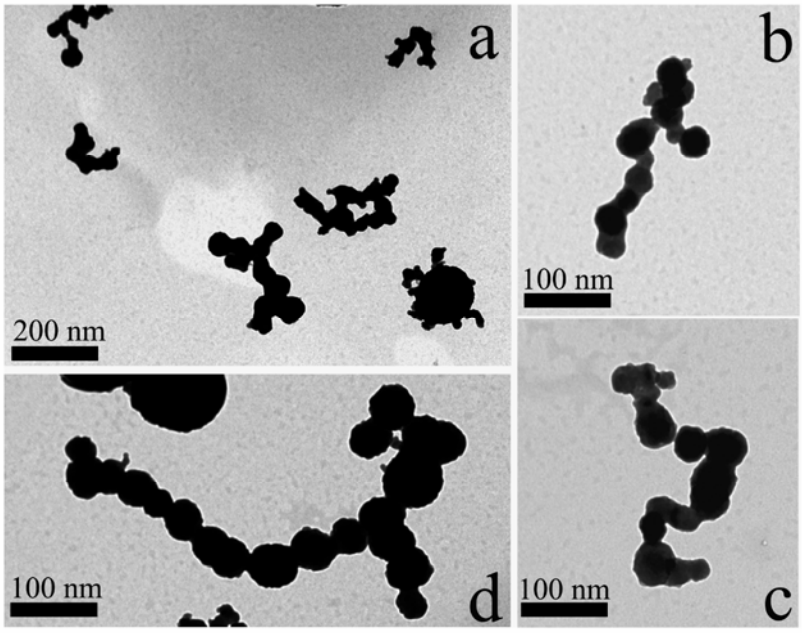

Figure 2. Typical (a) low and (b), (c), (d) higher magnification TEM images of synthesized products.

The formation of the Te 1D nanostructures (nanowires, nanotubes, nanobelts) through a vapour-solid (VS) growth mechanism is commonly reported in literature [7-9]. Typically, the growth of 1D nanostructures

could be explained through the tendency of tellurium crystals to grow in the direction of the trigonal axis more readily than in any other direction [10]. Initially, the thermally evaporated Te atoms, coming from the evaporation of Te metal, were concentrated and supersaturated in the furnace until Te nuclei were formed and grew into crystalline nanoparticles. Since Te vapours were continuously introduced into the tube furnace, Te atoms were continuously supplied. Because of the anisotropic crystal structure of tellurium, atoms deposited preferentially onto the (001) facet of the nanoparticles due to the difference of free energies of the various surfaces, yielding nanowires/nanotubes growth [10].

In the present study, Te nanoparticles assemblies could be observed only at a position farther away from the source (20cm away from the Te source). As we reported in a previous work, at a distance of 12cm from the source powder along the downstream side of the flowing gas, it was possible to observe the formation of microtubes [6]. In a conventional tube furnace, as the source-to-substrate distance increases, the concentrations of the evaporated species decrease gradually and the growth takes place much slower due to the limited amount of source material. Hence, for substrates closer to the source, the crystal growth is faster due to the abundant supply of the evaporated atoms in such a region [11]. At positions farther away from the source, the growth process is significantly slower, and this limits the crystal growth into larger sizes although nucleation would still occur as long as supersaturation is reached. This is consistent with the observation of large amount of nanocrystals with size ranging from 40 to 100nm. The self-assembly process of Te nanoparticles in necklace-like configuration could be explained as driven by the limited concentration of evaporated source and the reduction of surface energy. Although multiple nucleation is expected, lateral expansion of the nucleated Te nanoparticles is limited by the shortage in source supply from the vapour phase. Such an assembly process is similar to that proposed by Wang et al. in the synthesis of CdTe nanorods via the self-assembly of CdTe nanocrystals by

a catalyst-free thermal chemistry method [11]. In such a mechanism, the surfaces of nucleated nanoparticles could further serve as accommodating planes, allowing another Te nucleus to attach to it (assembly process) and resulting in the reduction in the surface energy of the nanocrystal nuclei.

On the other hand, the formation of bigger nanoparticles with short rods extruding from their surface could be also occasionally observed. This observation allows supposing that the process of self-assembly of nanoparticles into chains continued till the nanoparticles reached a minimum size which enabled the growth of nanorods from their surfaces.

3.2. UV-Vis and Raman characterization

In Figure 3(a), the UV-Vis absorption spectrum of tellurium nanochains show two characteristic peaks. Peak I is located at 330nm and it is due to the transition from p-bonding valence band to the p-antibonding conduction band. Peak II is located at 690nm and it is due to the transition from p-lone pair valence band to the p-antibonding conduction band [12].

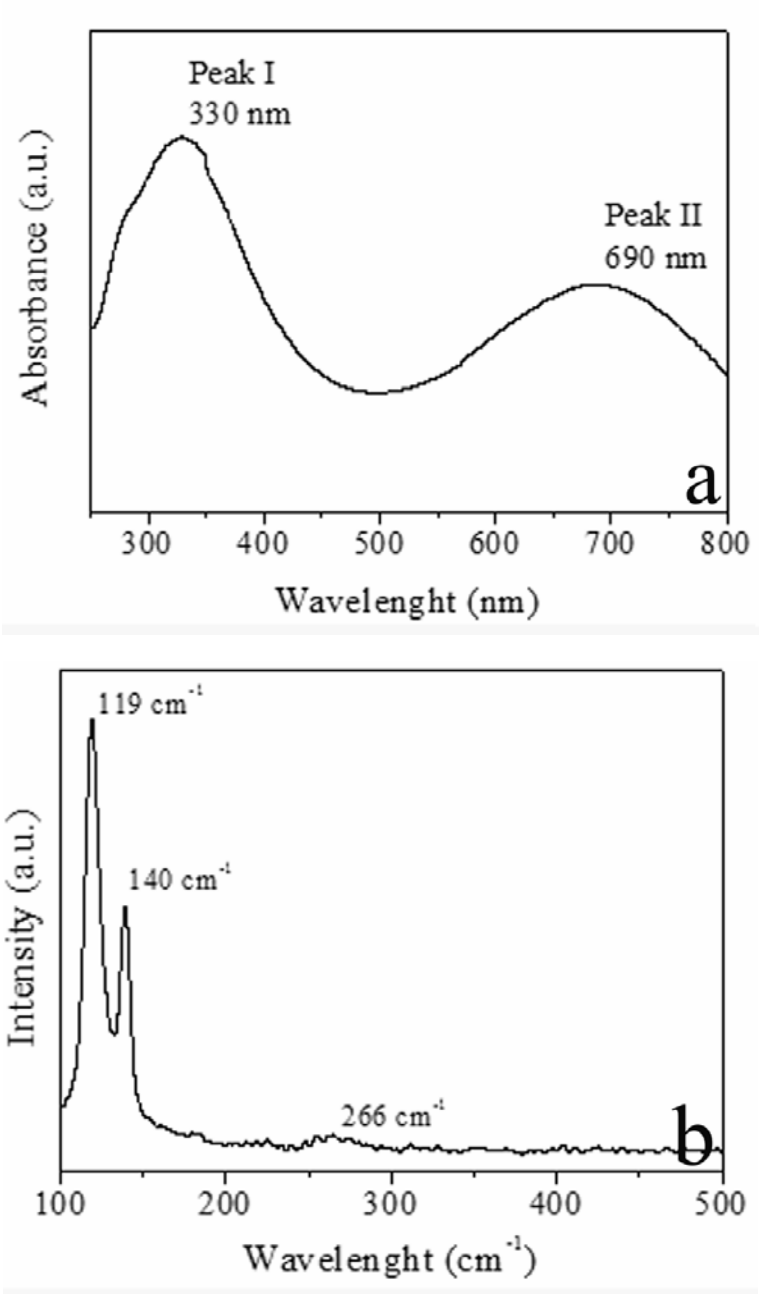

Figure 3. Typical (a) UV-Vis and (b) Raman spectrum of Te nanochains.

A typical Raman spectrum of Te products is reported in Figure 3(b). It is evident that the spectra show peaks at 119, 140, and 266cm^{-1}. The peaks at 119 and 140cm^{-1} can be assigned to A_1 and E phonon vibration modes of Te [13]; the peak at 266cm^{-1} can be assigned to the Te-O vibration of thin oxide layer [14]. A shift toward lower values with respect to the values reported in literature (149 and 267cm^{-1}) could be attributed to the nanometric size of the particles.

4. Sensing Test of PVA-Te Composite Thin Film

Figure 4 shows the experimental set-up used for the investigating the optical response of the PVA-Te composite upon exposure to different organic vapour samples (VOCs). The set up consists of a sensor chamber, a light source (tungsten halogen lamp), an air and VOCs vapour supply system and a spectrometer. The optical responses were studied by analyzing the plasmonic characteristic changes of the PVA-Te composite film upon exposure to the air and air-VOCs vapour mixtures as a function of time. The change in the optical properties of the prepared sample is due to the physisorption or chemisorption of a particular analyte interacting with the surface.

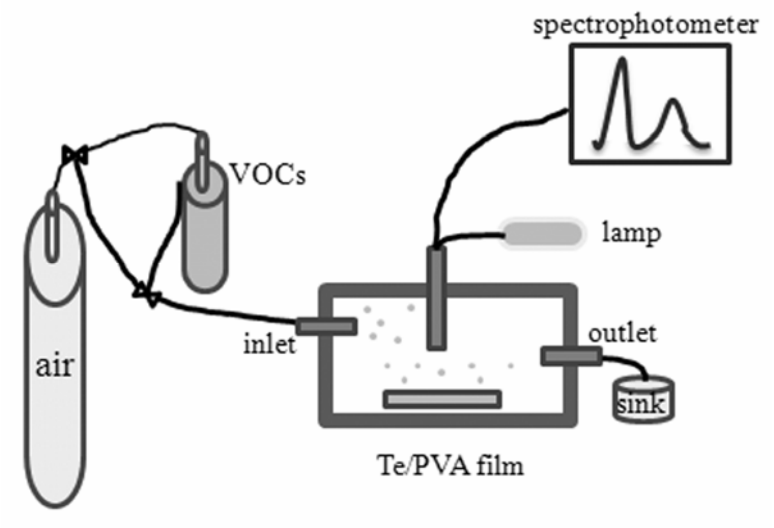

Figure 4. Experimental gas sensing system set-up.

Gas sensing performance of the prepared PVA-Te films to different organic vapour samples, such as methanol, ethanol, and 2-propanol has been tested. Figure 5 shows the real-time response of the composite films to different VOC gases, in which the concentration was increased from 4000 to 30000ppm. The change in the integral area (ΔI) calculated under the absorption curve in the range from 600 to 800nm is plotted. As shown, in all cases the interaction with organic vapour molecules produces an increase in the optical absorption signal with respect to that recorded in dry air. The signal saturates at higher analyte concentrations, possibly due to saturation of the available nanoparticle adsorption sites or to the filling of the available pore space within the film. From the response curves shown in Figure 5, the reversibility of the adsorption and desorption steps are clearly evident.

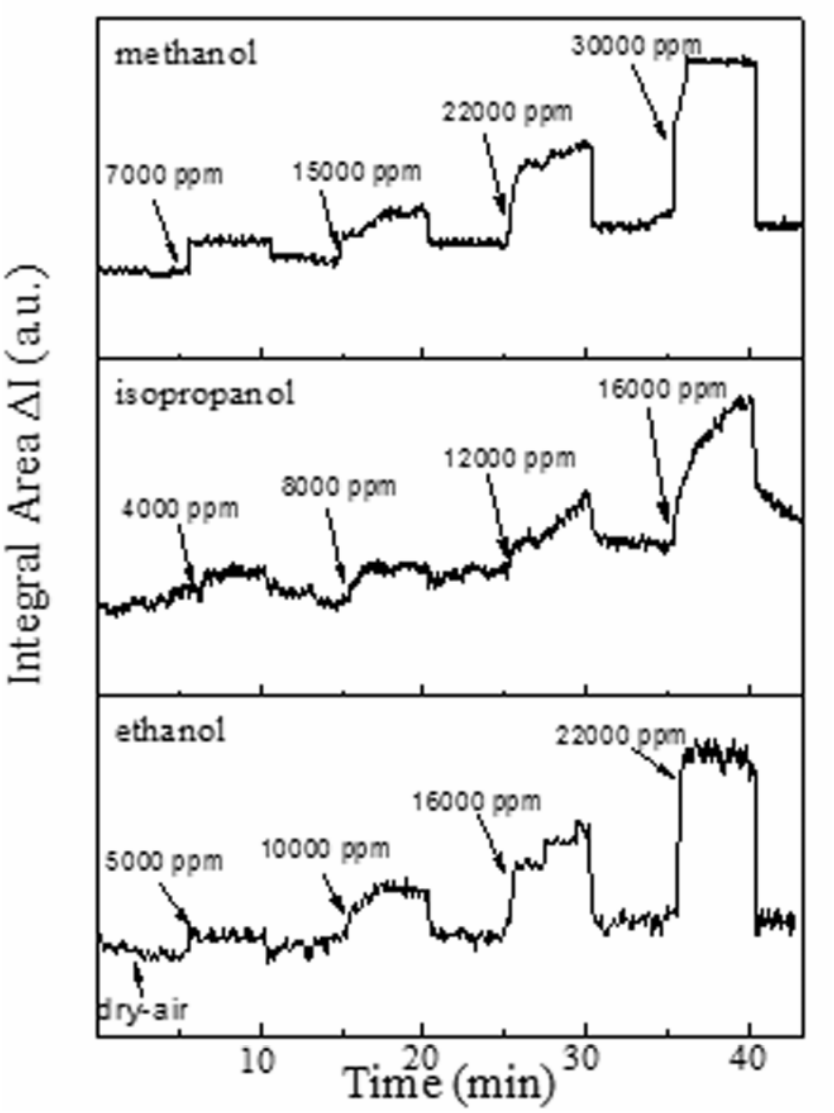

Figure 5. Dynamical surface plasmon resonance of the PVA-Te film for different methanol, isopropanol, and ethanol different vapours concentration in dry air.

The previous results suggest that when air containing a certain organic vapour sample flows into the gas chamber, the optical absorbance of the composite film in 600-800 wavelength range increases, reflecting a successful interaction between the vapour molecules and the samples. In spite of a high increase in the absorbance, the absorption spectrum returns to its initial condition when vapour is taken out of the gas chamber. It indicates that the vapour molecules might simply bind to the sample surface, probably, via a weak physical adsorption process such as Van der Waals interaction [15]. Hence, it is easily removed when a flow of air is purged into the sensing chamber. In Figure 6, the variations in the integrated absorption signal as a function of methanol, ethanol, and isopropanol vapours concentrations are reported. As one can see, the responses to methanol and isopropanol vapours are comparable and they are better than the response to ethanol vapours.

Based on these experimental results, it can be concluded that Te nanochains immobilized into PVA polymeric matrix were sensitive to the presence of VOC vapour samples. The optical response of the sample was also very stable by showing a gradual fluctuation in the response upon gas flowing in and out the sensing chamber.

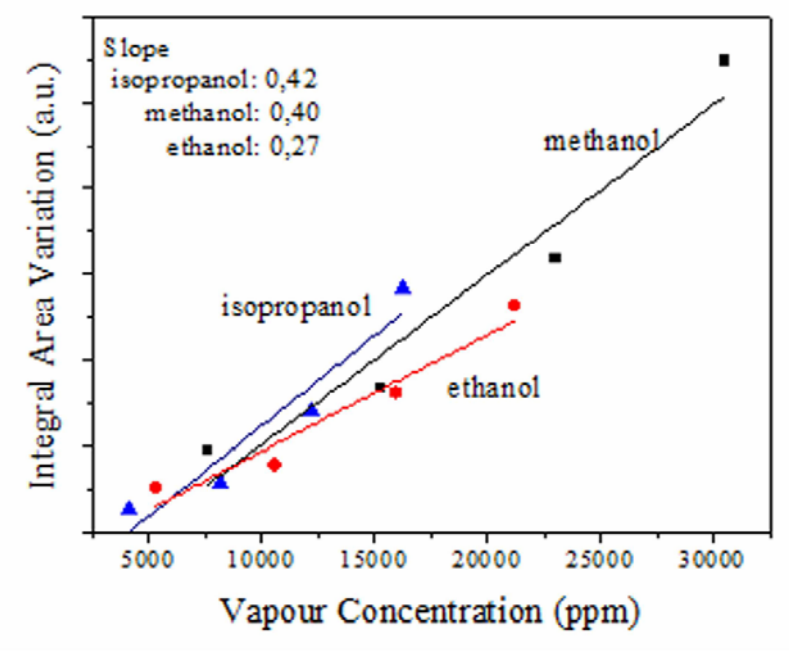

Figure 6. Variation in the integrated absorption signal as a function of methanol, ethanol, and isopropanol vapours concentrations.

As it has been mentioned earlier, the change in the absorption profiles of the prepared composite film upon exposure to the gas samples could be directly associated with the successful interaction between the film and the vapour molecules. Although the exact mechanism of such an interaction is not clear at this moment, it can be attributed to the modification of the dielectricity of the surrounding medium upon gas presence.

5. Conclusion

In the present work, we have proposed a physical vapour deposition route for synthesizing Te nanoparticles which self-assembled into chain-like structures. We confirmed Te nanoparticles formation and self-assembly using UV-Vis spectrometer and TEM technique, their crystalline nature

through XRD and Raman techniques. The simple synthetic approach described involved environmentally benign conditions with relatively low energy consumption and low temperature (500°C). To the best of our knowledge, the majority of the literature works concerning the preparation of Te nanostructures reported 1D growth (nanowires, nanobelts, nanotubes, …), since highly anisotropic crystalline structure of tellurium favours 1D nanostructured growth. We found that the distance from source powder, evaporating temperature and time were crucial factors in observing the self assembly mechanism of nanoparticles. In fact, the limited concentration of evaporated source is the key factor in the formation of necklace nanostructures. A hybrid PVA-Te nanochains thin film has been also developed through a simple and low cost strategy. The optical properties of PVA-Te nanochains film revealed an interesting tool for the detection of different alcohol vapours such as ethanol, methanol, and isopropanol.

References

[1] H. Wei and H. Eilers, Thin Solid Film, 517 (2008), 575.

[2] B. Zhang, W. Hou, X. Ye, S. Fu and Y. Xie, Adv. Funct. Mater. 17 (2007), 486.

[3] P. Mohanty, J. Park and B. Kim, Journal of Nanoscience and Nanotechnology 6 (2006), 1.

[4] X. Wu, Y. Wang, S. Zhou, X. Y. Yuan, T. Gao, K. Wang, S. Lou, Y. Liu and X. Shi, Cryst. Growth Des. 13 (2013), 136.

[5] A. K. Sahoo, S. K. Srivastava and X. Shi, Cryst. Growth Des. 11 (2011), 1597.

[6] T. Siciliano, E. Filippo, A. Genga, G. Micocci, M. Siciliano and A. Tepore, Cryst. Res. Technol. 46 (2011), 765.

[7] P. Mohanty, T. Kang, B. Kim and J. Park, J. Phys. Chem. B 110 (2006), 791.

[8] B. Geng, Y. Lin, X. Peng, G. Meng and L. Zhang, Nanotechnology 14 (2003), 983.

[9] Q. Wang, G. Dong Li, Y. L. Liu, S. Xu, K. J. Wang and J. S. Chen, J. Phys. Chem. C 11 (2007), 12926.

[10] J. Yuan, H. Schmalz, Y. Y. Xu, N. Miyajima, M. Drechsler, M. W. Moller, F. Scacher and A. H. E. Muller, Adv. Mater. 20 (2008), 947.

[11] X. N. Wang, J. Wang, M. J. Zhou, H. Wang, X. D. Xiao and Q. Li, Journal of Crystal Growth 312 (2010), 2310.

[12] A. K. Samal and T. Pradeep, J. Phys. Chem. C 113 (2009), 13539.

[13] R. Ochoa Landin, O. Vigil Galan, Y. V. Vorobiev and R. Ramirez Bon, Solar Energy 83 (2009), 134.

[14] A. K. Samal and T. Pradeep, J. Phys. Chem. C 113 (2009), 13539.

[15] S. Nengsih, A. A. Umar, M. M. Salleh and M. Yahaya, Sains Malaysiana 40 (2011), 231.

■